# Photoelectron spectroscopy of $Ti_n^-$ clusters ($n$=1–130)

Shu-Rong Liu and Hua-Jin Zhai
*Department of Physics, Washington State University, Richland, Washington 99352*
*and W. R. Wiley Environmental Molecular Sciences Laboratory, Pacific Northwest National Laboratory, MS K8-88, Richland, Washington 99352*

Miguel Castro
*Departamento de Física y Química Teórica, Facultad de Química Universidad Nacional Autonoma de México, Del. Coyoacán Cd. Universitaria, C. P. 04510, México D. F., México*

Lai-Sheng Wang[a)]
*Department of Physics, Washington State University, Richland, Washington 99352*
*and W. R. Wiley Environmental Molecular Sciences Laboratory, Pacific Northwest National Laboratory, MS K8-88, Richland, Washington 99352*

(Received 13 September 2002; accepted 1 November 2002)

Photoelectron spectra of cold $Ti_n^-$ anion clusters for $n$=1–130 were investigated at four detachment photon energies: 532, 355, 266, and 193 nm. Improved spectral resolution provides well-resolved electronic structures of the clusters, and the spectral evolution as a function of cluster size was probed systematically. Narrow and well-resolved spectral features were observed at $n$=13, 19, and 55, consistent with the high symmetry icosahedral structures proposed for these clusters. The measured electron affinities as a function of size in the studied size range do not extrapolate to the bulk work function, indicating that Ti clusters with $n$=130 may not assume the bulk structure. © *2003 American Institute of Physics.* [DOI: 10.1063/1.1531999]

## I. INTRODUCTION

It is a central theme in cluster science to probe the evolution of the electronic, structural and magnetic properties of metal clusters as a function of cluster size. Studies on the structural and electronic properties of transition metal (TM) clusters are essential to understand their detailed physical and chemical properties. However, due to the open *d* shells, TM clusters possess very complicated electronic structures and high density of electronic states and studies on the properties of TM clusters have posed tremendous challenges both experimentally and theoretically.[1]

Photoelectron spectroscopy (PES) of size-selected anions has emerged as a powerful experimental technique in providing information about the electronic structure and excitation energies of atomic clusters. Comparison of experimental PES data with theoretical calculations has become a valuable means to determine the structures and low-lying isomers for a variety of clusters.[2–7] However, due to their complexity, few such studies have been devoted to the TM clusters.[2,5] Experimentally, the dense low-lying electronic states of TM clusters have generally resulted in rather diffuse PES spectra.[8] Only very recently have we been able to obtain well-resolved PES data for TM clusters,[9,10] as a result of improved experimental resolution and the ability to produce colder clusters,[6,11] opening an avenue for a more precise comparison between the experimental spectra and computed density of states (DOS).

Studies on the properties of Ti clusters are relatively scarce compared to that of other TM clusters.[1] Collision-induced dissociations of $Ti_n^+$ ($n$=2–22) clusters have been reported.[12] A PES study was conducted previously in our group on $Ti_n^-$ clusters from $n$=3 to 65 at 266 nm.[13] Only one PES band was observed above $n$=8 under the previous experimental conditions and that observation was interpreted as an onset of the *d* band by comparing with bulk PES data. Theoretical studies using density functional theory (DFT) were carried out for small $Ti_n$ ($n$=2–10) and $Ti_n$ ($n$=2–14, 19, 55) clusters.[14,15] There has also been a study on $Ti_n$ ($n$=2–16) clusters using molecular dynamics.[16]

We have undertaken a more comprehensive PES study of $Ti_n^-$ clusters ($n$=1–130) under well-controlled experimental conditions and at various photon energies, 532, 355, 266, and 193 nm. The low photon energy data reveal more details of the electronic features of the small $Ti_n$ clusters, whereas the high photon energy spectra probe more deeply into the valence band of the clusters. In the accompanying paper,[17] we report a theoretical study on $Ti_n^-$ and $Ti_n$ ($n$=3–8, 13) and compare the theoretical results with the experimental data. The good agreement between the PES data and the calculated DOS allowed us to establish the ground states and low-lying isomers of $Ti_n^-$ and $Ti_n$ and provided insight into their structural and magnetic properties. In the present paper, we report the detailed PES results and the evolution of the electronic properties of Ti clusters from one atom up to 130 atoms at four detachment wavelengths with well-controlled cluster temperatures. Evidence of clusters with high symmetries and the *s/d* nature of the PES features will be presented. Electron affinities (EAs) of the neutral clusters from atomic Ti to $Ti_{130}$ and a possible structural transition will also be reported and discussed.

a)Author to whom correspondence should be addressed. Electronic mail: ls.wang@pnl.gov

 

## II. EXPERIMENT

### A. Experimental setup

The experiment was performed using a magnetic-bottle time-of-flight PES apparatus with a laser vaporization cluster source. Detailed descriptions about the apparatus were reported elsewhere.[8,18] A pulsed laser beam from a Nd:YAG laser (532 nm) was used to vaporize a pure Ti disk target. The laser-generated plasma was mixed with an intense high-pressure helium carrier gas pulse. Clusters formed in the nozzle were entrained in the carrier gas and underwent a supersonic expansion. Negatively charged clusters in the beam were extracted perpendicularly into a time-of-flight mass spectrometer. A given cluster of interest was mass selected and decelerated before photodetachment. In the present study, four detachment photon energies were used from a Nd:YAG laser at 532 nm (2.331 eV), 355 nm (3.496 eV), and 266 nm (4.661 eV) and an ArF excimer laser at 193 nm (6.424 eV).

We studied $Ti_n^-$ clusters previously for $n=3-65$ at 266 nm.[13] In the current study, several improvements were made. First, the instrumental resolution was slightly improved to ~2.5% ($\Delta E_k/E_k$), i.e., ~25 meV for 1 eV electrons, as measured from the known spectra of $Rh^-$. Second, we obtained data at four different photon energies, as mentioned above. The various photon energy data not only provide better spectroscopic information, but also provide insight into the nature of the photodetachment transitions from their intensity variations. Third, we have extended the cluster size to $n=130$ by fully optimizing the source conditions and mass spectrometer. Finally and most importantly, we have obtained data under well-controlled temperature conditions, as described below.

### B. Temperature effects

As shown previously for $Al_n^-$ cluster,[6,7,19] we found that the cluster temperature from our cluster source spans a wide range, depending on the residence time of the clusters in the nozzle and the firing timing of the vaporization laser.[11] To obtain cold clusters, we need to carefully tune the vaporization laser firing timing and the cluster residence time. We found that clusters coming out of the nozzle late tend to be colder. Significant temperature effects were observed for a large size range and wide temperature range. Hot clusters, in general, result in congested spectra that smear out discrete electronic transitions even under a high instrumental resolution. Spectra from cold clusters give rise to sharper spectral features, affording a definitive spectroscopic signature of the electronic structures of the underlying clusters.

Another important parameter also crucial for obtaining well-resolved PES spectra is the photon fluence of the detachment laser. High photon fluences result in multiphoton absorption and thermionic effects.[20] Sharp features would be smeared out by the thermally excited electronic states and by slow electrons from thermionic emissions. Figure 1 shows a set of temperature-dependent PES spectra of $Ti_{13}^-$. The three spectra were measured at different residence times with a fixed photon fluence of 0.05 mJ/cm$^2$. The hot spectrum in Fig. 1(a) corresponds to clusters leaving the nozzle early

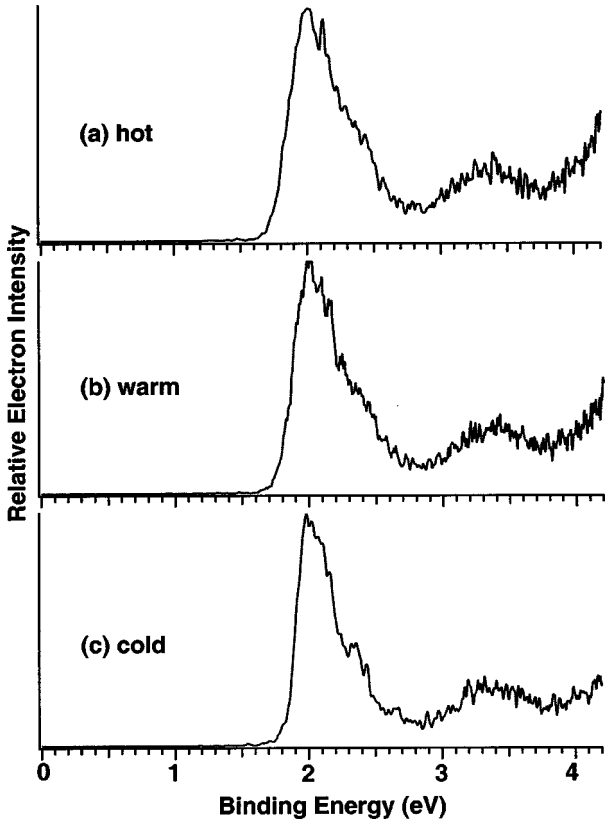


FIG. 1. Temperature effect on the photoelectron spectra of $Ti_{13}^-$. Photon energy, 266 nm (4.661 eV); photon fluence, 0.05 mJ/cm$^2$.

(short residence time). The spectra in Figs. 1(b) and 1(c) correspond to clusters with increasingly longer residence time. It is clear that the spectra were sharpened as the residence time was increased. The PES threshold also became better defined and increased to higher binding energies due to the reduction of hot band transitions. The thermionic effect is also clearly shown in the ''hot'' spectrum [Fig. 1(a)], as indicated by the high binding energy tail (corresponding to low energy electrons). Figure 2 illustrates both the temperature and photon-fluence effects on the PES spectra of $Ti_{55}^-$. On the left column, a photon fluence of 0.01 mJ/cm$^2$ was used while the residence time was increased from Fig. 2(a) to Fig. 2(c), a similar spectral improvement was observed as that shown in Fig. 1. On the right column, the residence time was kept the same as that in Fig. 2(b), while the photon fluence was varied. Clearly, high photon fluences yielded broader spectra due to multiphoton absorption that tends to ''heat'' up the cluster anions.[20]

All the PES spectra reported in this study were obtained under optimal conditions by carefully controlling the cluster residence time (as long as possible) and detachment laser fluence (as low as possible).

## III. EXPERIMENTAL RESULTS

### A. Photoelectron spectra at 532 nm

The 532 nm PES spectra are shown in Fig. 3 for $Ti_n^-$ ($n=3-10$). Due to the increasing electron binding energies of the larger clusters, we did not investigate $Ti_n^-$ clusters for

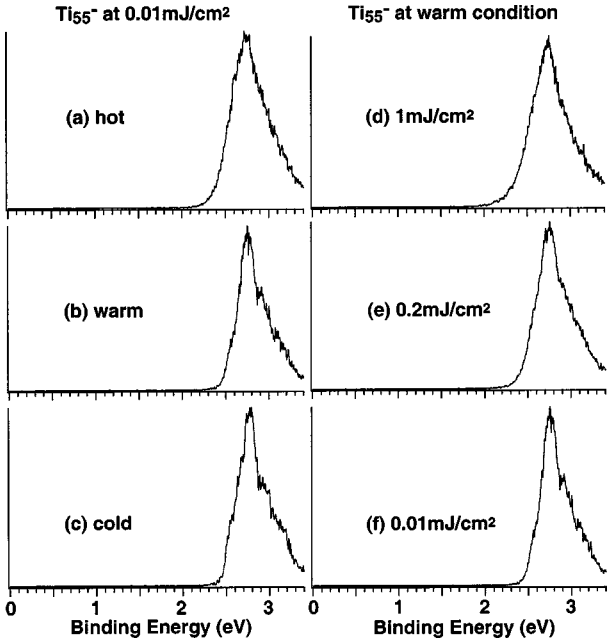


FIG. 2. Temperature and photon fluence effects on the photoelectron spectra of $Ti_{55}^-$. Photon energy, 355 nm (3.496 eV).

$n>10$ at this low photon energy. The 532 nm spectra represent the best resolved data. Fine features in the lower binding energy range were well resolved, revealing the discrete electronic energy levels of the neutral clusters. Relatively sharp peaks were observed at the threshold for all clusters except for $Ti_3^-$ and $Ti_6^-$. The weak low energy tail in all the spectra was due to hot band transitions, indicating that all cluster anions still had finite temperatures even under our best conditions. Since no vibrational structures were resolved, we estimated the adiabatic detachment energies (ADEs) or the EAs of the neutral cluster by drawing a straight line at the leading edge of the threshold feature and then added a constant to the intersection with the binding energy axis to take into account the instrumental resolution. The relatively sharp peaks allowed us to obtain rather accurate EA values for these clusters as given in Table I.

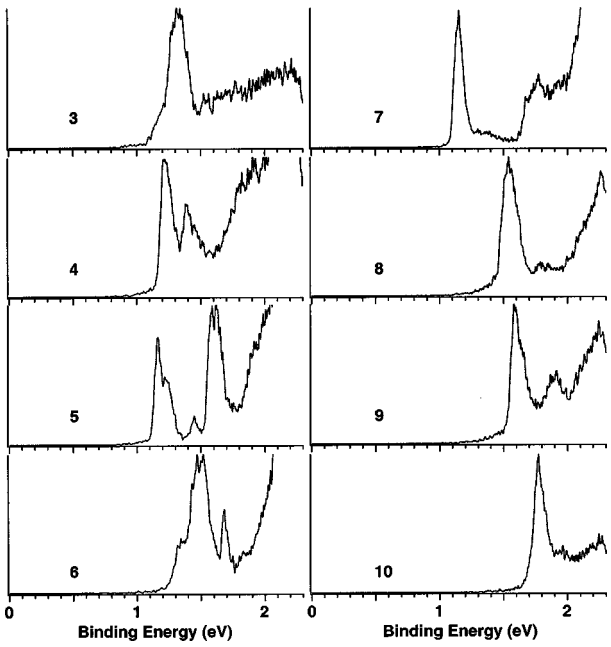


FIG. 3. Photoelectron spectra of $Ti_n^-$ ($n=3$–10) at 532 nm (2.331 eV).

### B. Photoelectron spectra at 355 nm

The 355 nm spectra are shown in Figs. 4 and 5 for $Ti_n^-$ ($n=1$–100). The Ti atom has an extremely low EA, as shown previously.[21] The $Ti_2^-$ dimer mass intensity was too weak under our source conditions for us to measure its PES spectrum. Figure 4 reveals that clusters smaller than 10 atoms exhibit very different PES spectra without resemblance to each other, underlying their molecular nature. A spectral transition, from a complicated multipeak spectrum to a seemingly simpler spectrum dominated by a sharp and intense threshold peak, happened from $Ti_9^-$ to $Ti_{10}^-$. The spectrum of $Ti_{11}^-$ shows a second band at ~2.3 eV. The spectrum of $Ti_{12}^-$ has a single band with discernable fine features, whereas that of $Ti_{13}^-$ seems special with a single and rather narrow band. The spectrum of $Ti_{14}^-$ shows some similarities to that of $Ti_{13}^-$ except that it is broader with a shoulder on each side of the main peak. The spectrum of $Ti_{15}^-$ shows some resemblances to that of $Ti_{14}^-$. The spectrum of $Ti_{16}^-$ is quite different from that of $Ti_{15}^-$: it shows two features with almost equal widths and intensities. Surprisingly a sharp threshold peak was resolved in the spectrum of $Ti_{17}^-$ and $Ti_{19}^-$, but not in that of $Ti_{18}^-$. The spectrum of $Ti_{20}^-$ appears similar to that of $Ti_{18}^-$, whereas those from $Ti_{21}^-$ to $Ti_{23}^-$ became broader without clearly resolved features. Sharp threshold peaks were also observed in the spectra of $n=24$–27. The spectra of $Ti_{28}^-$ and $Ti_{29}^-$ are similar to each other with two resolved bands. The spectra of $Ti_{30}^-$ and $Ti_{31}^-$ also show discernable fine features, but beyond $Ti_{31}^-$, the PES spectra show no well-resolved features and became one broad band. The 355 nm spectra for $Ti_{33}^-$ to $Ti_{100}^-$ are displayed in Fig. 5, where only a broad and featureless band was observed for all clusters. The only exception is $Ti_{55}^-$, which gave a relatively narrow PES band with discernible fine features. Beyond $Ti_{66}^-$, we only recorded PES data at selected cluster sizes due to the spectral similarity of the large clusters. The EAs for $n=11$–100 were obtained from the 355 nm spectra, as given in Table I.

### C. Photoelectron spectra at 266 nm

The 266 nm PES spectra of $Ti_n^-$ ($n=3$–56) are shown in Fig. 6. These data in general are better resolved than what we reported previously at the same photon energy,[13] due to the improved experimental conditions mentioned above. The spectrum of $Ti_{13}^-$ shows a resolved shoulder on the high-energy side of the main peak. This feature was not observed clearly in the 355 nm spectrum. The low binding energy shoulder of the $Ti_{14}^-$ spectrum observed at 355 nm was smeared out due to the deteriorated energy resolution at the higher photon energy, but the intensity of the high binding energy shoulder was enhanced compared to that in the 355 nm spectrum. Interestingly, the 266 nm PES spectra of $Ti_{12}^-$ to $Ti_{15}^-$ appear similar to that of $Ti_{13}^-$ still being relatively narrow. Overall, the 266 nm data are consistent with the 355 nm data. The special nature of $Ti_{55}^-$ is again revealed in the

TABLE I. Adiabatic electron affinity (EA) of $Ti_n$ clusters ($n$=1–130).

| $n$ | EA (eV) | $n$ | EA (eV) | $n$ | EA (eV) |
|---|---|---|---|---|---|
| 1 | 0.080±0.014[a] | 27 | 2.14±0.05 | 52 | 2.41±0.05 |
| 3 | 1.13±0.06 | 28 | 2.14±0.05 | 53 | 2.41±0.06 |
| 4 | 1.18±0.03 | 29 | 2.12±0.05 | 54 | 2.45±0.06 |
| 5 | 1.15±0.03 | 30 | 2.16±0.05 | 55 | 2.51±0.05 |
| 6 | 1.28±0.05 | 31 | 2.19±0.05 | 56 | 2.48±0.06 |
| 7 | 1.11±0.03 | 32 | 2.24±0.05 | 57 | 2.49±0.05 |
| 8 | 1.47±0.05 | 33 | 2.21±0.05 | 58 | 2.47±0.05 |
| 9 | 1.56±0.05 | 34 | 2.22±0.06 | 59 | 2.49±0.05 |
| 10 | 1.70±0.05 | 35 | 2.24±0.05 | 60 | 2.51±0.06 |
| 11 | 1.72±0.05 | 36 | 2.24±0.05 | 61 | 2.55±0.05 |
| 12 | 1.71±0.05 | 37 | 2.27±0.05 | 62 | 2.57±0.05 |
| 13 | 1.87±0.05 | 38 | 2.28±0.06 | 63 | 2.57±0.05 |
| 14 | 1.87±0.05 | 39 | 2.29±0.05 | 64 | 2.60±0.05 |
| 15 | 2.00±0.05 | 40 | 2.34±0.06 | 65 | 2.55±0.05 |
| 16 | 1.96±0.05 | 41 | 2.33±0.05 | 66 | 2.58±0.05 |
| 17 | 2.01±0.05 | 42 | 2.32±0.05 | 70 | 2.55±0.06 |
| 18 | 1.97±0.05 | 43 | 2.36±0.05 | 75 | 2.63±0.06 |
| 19 | 1.93±0.05 | 44 | 2.39±0.05 | 80 | 2.68±0.06 |
| 20 | 2.06±0.05 | 45 | 2.40±0.05 | 90 | 2.66±0.06 |
| 21 | 1.98±0.05 | 46 | 2.39±0.05 | 100 | 2.73±0.06 |
| 22 | 2.04±0.05 | 47 | 2.41±0.05 | 110 | 2.75±0.08[b] |
| 23 | 2.08±0.05 | 48 | 2.44±0.05 | 120 | 2.75±0.08[b] |
| 24 | 1.97±0.05 | 49 | 2.40±0.05 | 130 | 2.83±0.08[b] |
| 25 | 2.07±0.05 | 50 | 2.38±0.05 | | |
| 26 | 2.10±0.05 | 51 | 2.41±0.05 | | |

[a]From Ref. 21.
[b]The masses of these clusters were not well separated and were estimated with an error of several atoms ($n$±4).

266 nm data. Large clusters beyond $Ti_{56}^-$ were not measured at 266 nm because a more systematic data set was obtained at 193 nm (see Fig. 7). At 266 nm, the most significant observation is the appearance of the PES band starting from $\sim Ti_{12}^-$ at around 3 eV. This band has relatively weak intensity and shifts gradually to higher binding energies with the increase of the cluster size. In our previous study on the Ti clusters at 266 nm,[13] this additional spectral feature was not clearly observed due to the relatively hot clusters and perhaps high detachment photon fluxes, which both tended to enhance thermionic emissions and smeared out the higher binding energy feature.

### D. Photoelectron spectra at 193 nm

The 193 nm spectra of $Ti_n^-$ ($n$=4–130) are shown in Fig. 7. Although the spectral resolution deteriorated compared to the lower photon energy spectra, the 193 nm data revealed the electronic structure in a wider energy range. Starting from $Ti_{12}^-$, the second PES band was clearly revealed at around 3.3 eV. Significant electron signals were also observed at higher binding energies and the spectra became almost continuous in the higher binding energy side from $Ti_{20}^-$ to $Ti_{80}^-$. However, the continuous spectral features were replaced with a well shaped spectral band around 4.5 eV from $Ti_{90}^-$ to $Ti_{130}^-$. Due to the isotope distributions and the limited mass resolution, the spectra of the large clusters over 100 atoms contained a range of cluster sizes of $n\pm4$. The EAs of $Ti_{110}$, $Ti_{120}$, and $Ti_{130}$ were estimated from the 193 nm spectra, as given in Table I.

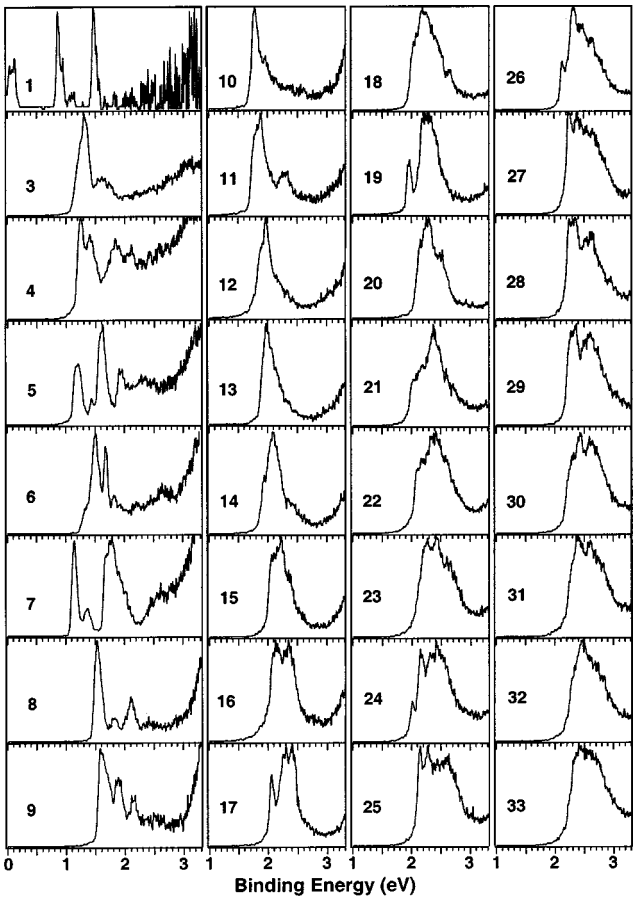


FIG. 4. Photoelectron spectra of $Ti_n^-$ ($n$=1–33) at 355 nm.

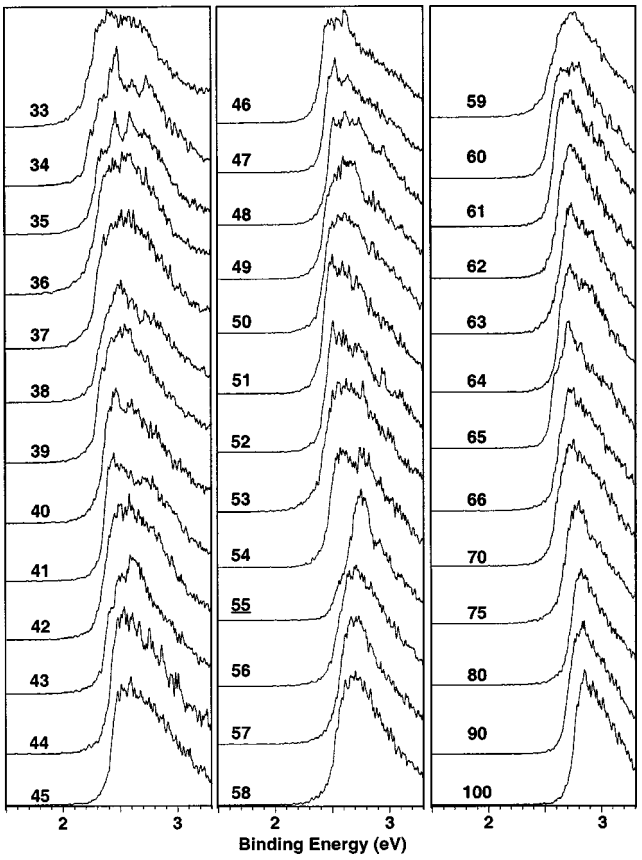


FIG. 5. Photoelectron spectra of $Ti_n^-$ ($n$=33–100) at 355 nm.

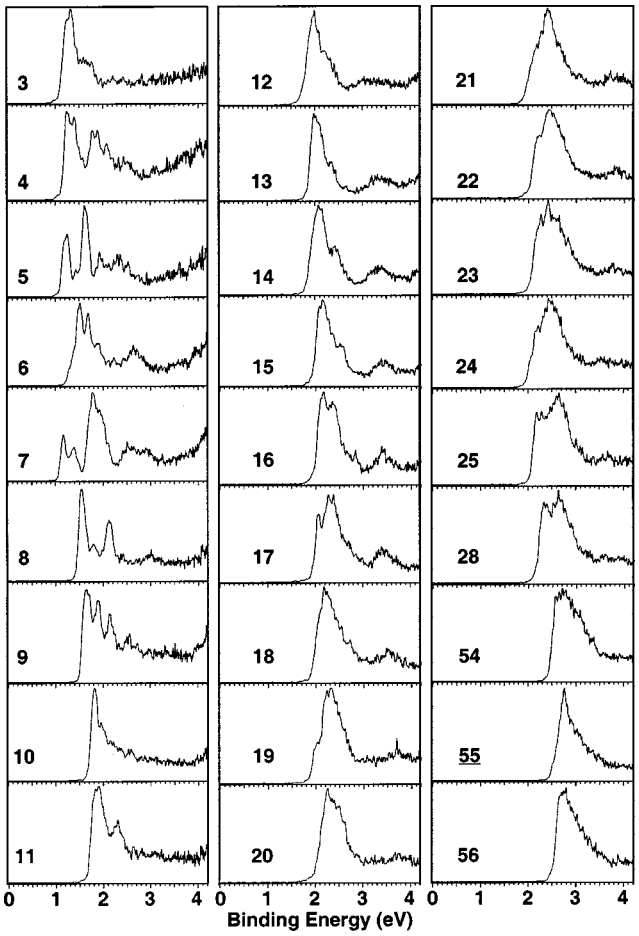


FIG. 6. Photoelectron spectra of $Ti_n^-$ ($n$=3–56) at 266 nm.

Within the experimental uncertainty, the EAs obtained in the current study (Table I) are consistent with our previous results in the size range of $Ti_3$ to $Ti_{65}$. The better spectral resolution in the current experiment resulted in slightly more accurate EAs.

### E. Photon energy dependent PES spectra

Figure 8 shows the PES spectra of $Ti_7^-$ and $Ti_8^-$ at four photon energies in the same energy scale. The spectra of $Ti_7^-$ and $Ti_8^-$ exhibit similar features with similar photon energy dependence. For example, the relative intensities of peak *A* in both systems decreased with the increase of photon energies, whereas those of features *B* and *C* increase with the increase of photon energies. Figure 9 displays the PES spectra of $Ti_{25}^-$ and $Ti_{28}^-$ at three photon energies. It was observed that for these two systems the relative intensities of the lower binding energy features decreased with increasing photon energies. Such photon energy dependence provides information about the nature of the electrons being detached and will be further discussed later.

## IV. DISCUSSION

### A. Evidence of highly symmetric clusters

In the accompanying paper,[17] a combination of PES and theoretical study is reported on small Ti clusters, $Ti_3^-$ to $Ti_8^-$, and $Ti_{13}^-$. Detailed electronic and structural information was obtained for these clusters based on the good agreement between the computational and experimental results. We have previously observed structure effect on photoelectron spectra for several 13-atom clusters. In our study of $Al_n^-$ clusters,[19] we observed an abrupt change in the PES spectra from a complicated multifeature spectrum for $Al_{12}^-$ to a simple single band for $Al_{13}^-$, which was confirmed to be an ideal icosahedron through a combined experimental and theoretical study.[6,7] The PES spectra of $Al_{14}^-$ and $Al_{15}^-$ maintained the main feature of $Al_{13}^-$ and these clusters were shown to be capped icosahedra. $Al_{16}^-$ gave a quite different PES spectrum, indicating a significant structural transition from $Al_{15}^-$ to $Al_{16}^-$. In Co and Ni clusters, we made similar observations about abrupt PES spectral changes and highly symmetric clusters.[9,10,22] For example, the PES spectrum of $Co_{13}^-$ became very sharp compared to that of $Co_{12}^-$, consistent with the icosahedral structure suggested for $Co_{13}^-$. The spectra of $Co_{14}^-$ and $Co_{15}^-$ were similar to that of $Co_{13}^-$, except that they are slightly more diffuse; similar icosahedral structures with one or two capping atoms were possible arrangements for $Co_{14}^-$ and $Co_{15}^-$. Abrupt PES spectra change from $Co_{15}^-$ to $Co_{16}^-$ marks a possible structural transition from the icosahedral packing.[9]

An ideal icosahedron was proposed for $Ti_{13}$ previously.[15] Using DFT calculations, we obtained a slightly distorted icosahedron structure for $Ti_{13}^-$ and $Ti_{13}$.[17] Based on the simi-

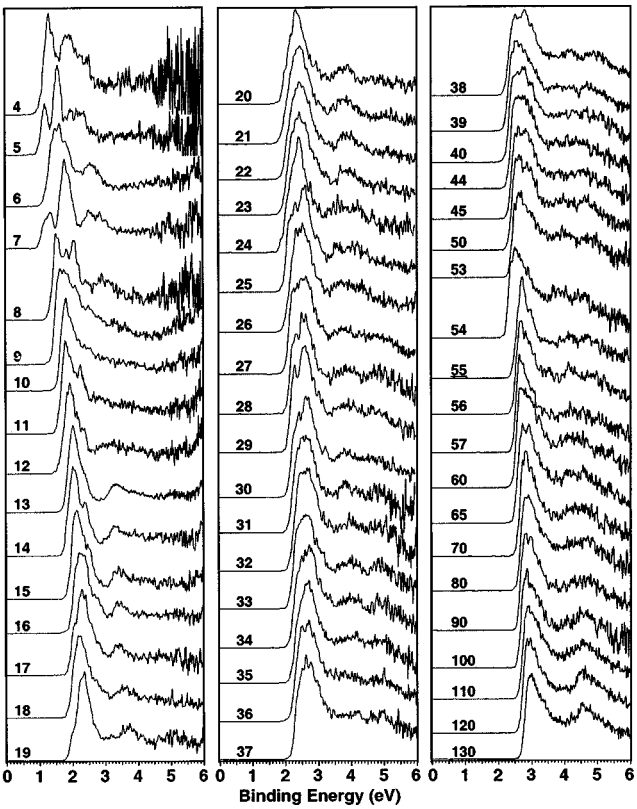


FIG. 7. Photoelectron spectra of $Ti_n^-$ ($n$=4–130) at 193 nm (6.424 eV).

larity of the PES spectra of $Ti_{14}^-$ and $Ti_{15}^-$ to that of $Ti_{13}^-$, a similar conjecture as for Al or Co clusters, could be drawn for the Ti clusters. $Ti_{14}^-$ and $Ti_{15}^-$ may also possess icosahedral geometry with one or two capping atoms. In fact, the icosahedral packing may extend to even larger clusters on the basis of their similar PES spectra to the basic pattern of the $Ti_{13}^-$ PES spectra. Additional evidence of high symmetry clusters was also observed in other size regime. As seen in Fig. 4, the PES spectra from $Ti_9^-$ to $Ti_{10}^-$ display a transition from a complex multipeak spectrum to a relatively simple one, indicating that a structural transition might exist

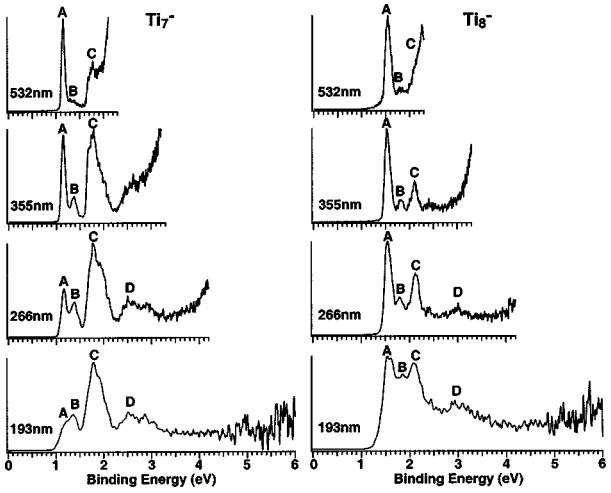


FIG. 8. Photoelectron spectra of $Ti_7^-$ and $Ti_8^-$ at four detachment photon energies.

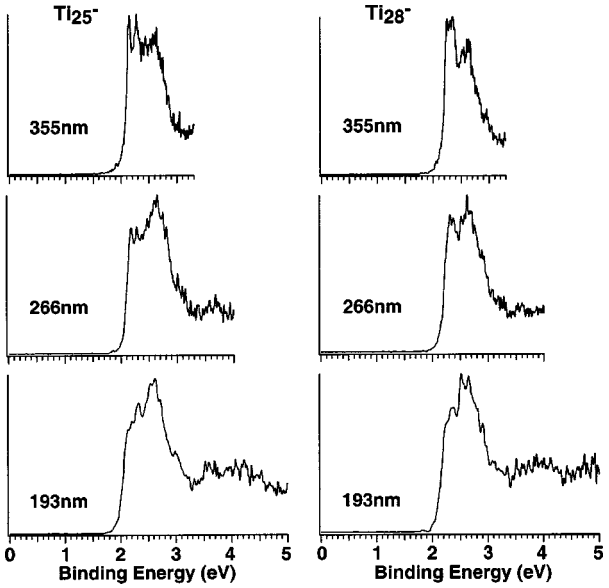


FIG. 9. Photoelectron spectra of $Ti_{25}^-$ and $Ti_{28}^-$ at three detachment photon energies.

from $Ti_9^-$ to $Ti_{10}^-$. $Ti_9^-$ may possess a less symmetric structure than $Ti_{10}^-$, consistent with a previous theoretical study, showing a $C_{1h}$, and $C_{3v}$ symmetry for $Ti_9$ and $Ti_{10}$, respectively.[14] In another theoretical study,[15] a bicapped and a tricapped pentagonal bipyramid structure were suggested for $Ti_9$ and $Ti_{10}$, respectively, and the structure of $Ti_{10}$ is again more symmetric.

Resolved sharp peaks at the threshold of the $Ti_{17}^-$ and $Ti_{19}^-$ spectra may also suggest a highly symmetric structure for these two clusters. The previous theoretical study[15] indicated a double icosahedral ground state structure for $Ti_{19}$, which was found to be 5.89 eV lower in energy than that of an octahedral structure. Theoretical structural information on $Ti_{17}^-$ and $Ti_{18}^-$ is not yet available. Nevertheless, from its highly resolved PES spectrum, a more symmetric structure for $Ti_{17}^-$ is likely.

In our previous studies, sharp peaks were resolved in the PES spectrum at and around $Co_{55}^-$, $Ni_{55}^-$, and $Fe_{55}^-$,[9,10,22,23] suggesting highly symmetric $I_h$ structures for these clusters. The PES spectra of $Ti_{55}^-$ at all three photon energies showed much better resolved features, quite distinct from those of its neighbors. This observation suggests that $Ti_{55}^-$ may also possess a highly symmetric $I_h$ structure. Indeed, a previous theoretical study found that the $I_h$ structure was 1.65 eV more stable than a cuboctahedron for $Ti_{55}$.[15]

### B. *s–d* hybridization and implication for the magnetic properties of Ti clusters

It is well established that small clusters of the late 3*d* elements possess localized 3*d* electrons, leading to enhanced magnetic moments.[1] Hybridization between the 4*s* and 3*d* orbitals was suggested to increase significantly as cluster size increases, resulting in reduced magnetic moments in larger

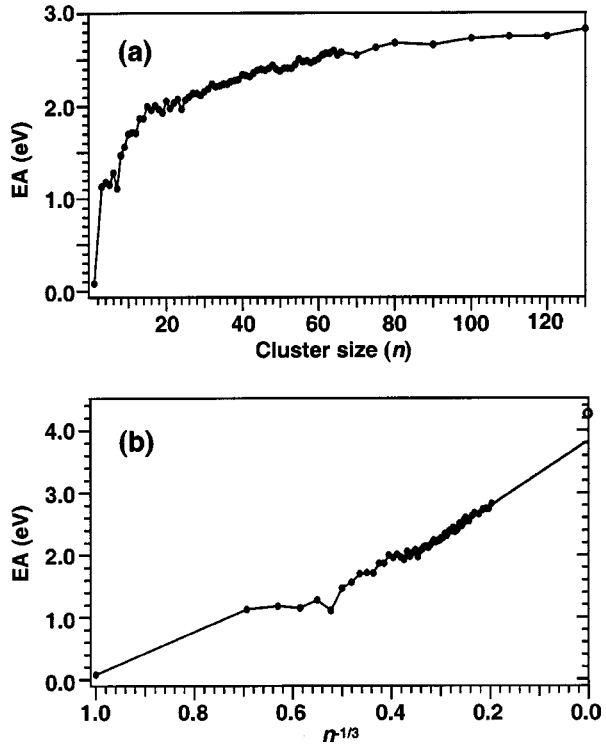


FIG. 10. (a) Electron affinities (EA) of $Ti_n$ as a function of $n$. (b) EA vs $n^{-1/3}$ (proportional to $1/r$, $r$ being the cluster radius). The unfilled circle indicates the bulk work function.

clusters.[10,24] The electronic structure of Ti clusters is expected to be different from those of the late 3*d* TM clusters because the 3*d* orbitals of Ti are delocalized valence orbitals. Therefore, *s/d* hybridization is expected for even the smallest Ti cluster and this should have significant effect on the magnetic properties of these clusters. Figure 8 shows the photon energy dependence of the detachment transitions of $Ti_7^-$ and $Ti_8^-$. Since detachment cross sections for different electrons (*s*, *p* or *d*) should have different photon energy dependence,[25] the peak intensity change provides information about the nature of the PES features. For both $Ti_7^-$ and $Ti_8^-$, the intensity of peak *A* decreases and the intensities of peaks *B* and *C* increase with the increase of photon energies, suggesting peak *A* should be from detachment of primarily *s* electrons and peaks *B* and *C* from primarily *d* electrons. This is consistent with our theoretical analysis of the DOS of these clusters. Our theoretical analysis revealed the complexity of the electronic structure of the Ti clusters and showed that, even for $Ti_7^-$, the energy levels of the *s* and *d* electrons are already mixed.[17] The delocalization and the bonding nature of the 3*d* electrons should result in dramatically reduced magnetic moments in small Ti clusters.[26]

Figure 9 shows that the intensities of the threshold PES features of $Ti_{25}^-$ and $Ti_{28}^-$ decrease with increasing photon energies. By comparing the spectra in Figs. 4–7, we note that a number of small $Ti_n^-$ clusters with well resolved threshold peaks show *s*-like behavior, whereas such photon energy dependence was largely unobservable in the large clusters, indicating the complete *s/d* hybridization in these systems. This observation is consistent with a previous Stern–Gerlach experiment, in which no measurable magnetic moments were detected for Ti clusters.[26]

### C. Electron affinity versus cluster size

Figure 10 shows the measured EAs of the $Ti_n$ clusters as a function of size. The EAs exhibit strong size variation in the smaller size regime from the atom to about $Ti_{25}$. Some of the EA variations in the large size regime correlate to structural effect. For example, the EA of $Ti_{55}$ exhibits a local maximum [Fig. 10(a)], which correlates to its highly symmetric structure mentioned above. Beyond $Ti_{25}$, the EAs essentially follow a straight line versus $1/n^{1/3}$, which is proportional to $1/r$, $r$ being the radius of the clusters [Fig. 10(b)]. According to the classical metallic droplet model,[27] the EAs of finite spherical metallic particles are proportional to $1/r$ and should extrapolate to the bulk work function at infinite $r$. However, the EA versus $1/n^{1/3}$ of the Ti clusters extrapolates to a value of around 3.80 eV at infinite size, which is significantly smaller than the bulk work function (4.33 eV) of a polycrystalline Ti film.[28] Previously, we have obtained consistent agreement between the extrapolated EAs at infinite size and the bulk work functions for all other TM cluster systems including V, Cr, Fe, Co, and Ni.[8,9,22,23,29,30] The disagreement between the extrapolated EA and the bulk work function in the Ti system might suggest that the Ti clusters in the studied size regime may possess structures other than the bulk and that there must be a structural transition at even larger sizes, from thereon the EA versus $1/n^{1/3}$ curve should exhibit a different slope.

### D. Comparison to other 3*d* metal clusters and further implications for cluster packing

The most interesting observation in the 193 nm spectra is the higher binding energy transitions starting from $Ti_{12}^-$, which emerge as a well-defined band starting from $Ti_{60}^-$. These spectral features are quite different from the bulk photoemission spectra of Ti, which only show a single band in the valence range.[31,32] However, we have observed previously for *V* clusters that PES spectra starting from $\sim V_{60}^-$ began to resemble those from the bulk body-centered-cubic (BCC) crystal.[29] Surprisingly, the two-band features observed for the PES spectra of the $Ti_n^-$ clusters are very similar to those observed for the V clusters.

Vanadium is next to Ti in the periodic table, but they have different bulk crystal structures. Vanadium has a BCC lattice, whereas Ti and the other group IVB elements (Zr and Hf) adopt the hexagonal-closed packed (HCP) lattice at room temperature. However, it is well known that there is HCP to BCC solid-to-solid phase transition for the group IVB metals at high temperatures.[33,34] In fact, there was a previous PES study of the HCP to BCC phase transitions for the Group IVB metals, but due to the low resolution of the experiment and the high temperature conditions, no observable difference was obtained between the BCC and HCP structures.[35] Our current observation of the similarity between the PES spectra of Ti clusters and those of *V* clusters might suggest that they both have similar cluster packing, i.e., the small Ti

clusters possess BCC-type structures, rather than the HCP-type structures. This conjecture is consistent with the EAs versus $1/n^{1/3}$ trend, which does not extrapolate to the bulk work function of the HCP crystal, as discussed above. The coldest clusters produced from our cluster source are around room temperature, as shown previously for small Al clusters.[6] Our current observation suggests that the HCP to BCC phase transition in small Ti clusters occurs at much lower temperatures than the bulk. This is a tentative conclusion, which warrants further theoretical verifications.

## V. CONCLUSIONS

We reported an extensive PES study of $Ti_n^-$ ($n$=1–130) clusters at four photon energies. Spectral evidence was observed for highly symmetric icosahedral $Ti_{13}^-$ and $Ti_{55}^-$, which both show an abrupt spectral narrowing compared to the PES spectra of their neighbors. Due to the improved experimental conditions, well resolved data were observed, allowing more details in the PES spectra to be obtained for the small clusters. The high photon energy data revealed high binding-energy valence-band transitions. It was shown that the EAs of the Ti clusters do not extrapolate to the bulk work function, indicating that the clusters in the observed size range may not possess the bulk packing. This observation is corroborated by the surprising observation that the PES spectra of the larger Ti clusters resemble those of V clusters, suggesting that the Ti clusters may possess BCC-type structures as the V clusters, rather than the HCP-type structure expected from the bulk lattice.

## ACKNOWLEDGMENTS

This work was supported by the National Science Foundation (CHE-9817811) and was performed at the W. R. Wiley Environmental Molecular Sciences Laboratory, a national scientific user facility sponsored by DOE's Office of Biological and Environmental Research and located at the Pacific Northwest National Laboratory, operated for DOE by Battelle. M.C. acknowledges financial support from CONACYT-México under Project 34845-E and from DGAPA–UNAM under Project PAPPIIT-IN-101901. The access to the supercomputer SG Origin 2000/32 at DGSCA–UNAM is greatly appreciated.

[1] J. A. Alonso, Chem. Rev. **100**, 637 (2000).
[2] C. Massobrio, A. Pasquarello, and R. Car, Phys. Rev. Lett. **75**, 2104 (1995).
[3] N. Binggeli and J. R. Chelikowsky, Phys. Rev. Lett. **75**, 493 (1995).
[4] J. Muller, B. Liu, A. A. Shvartsburg, S. Ogut, J. R. Chelikowsky, K. W. M. Siu, K. M. Ho, and G. Gantefor, Phys. Rev. Lett. **85**, 1666 (2000).
[5] H. Kietzmann *et al.*, Phys. Rev. Lett. **77**, 4528 (1996).
[6] J. Akola, M. Manninen, H. Hakkinen, U. Landman, X. Li, and L. S. Wang, Phys. Rev. B **60**, R11297 (1999).
[7] J. Akola, M. Manninen, H. Hakkinen, U. Landman, X. Li, and L. S. Wang, Phys. Rev. B **62**, 13216 (2000).
[8] L. S. Wang and H. Wu, in *Advances in Metal and Semiconductor Clusters. Vol. 4, Cluster Materials*, edited by M. A. Duncan (JAI, Greenwich, CT, 1998), p. 299.
[9] S. R. Liu, H. J. Zhai, and L. S. Wang, Phys. Rev. B **64**, 153402 (2001).
[10] S. R. Liu, H. J. Zhai, and L. S. Wang, Phys. Rev. B **65**, 113401 (2002).
[11] L. S. Wang and X. Li, "Temperature effects in anion photoelectron spectroscopy of metal clusters," in *Clusters and Nanostructure Interfaces*, edited by P. Jena, S. N. Khanna, and B. K. Rao (World Scientific, New Jersey, 2000), p. 293.
[12] L. Lian, C. X. Su, and P. B. Armentrout, J. Chem. Phys. **97**, 4084 (1992).
[13] H. Wu, S. R. Desai, and L. S. Wang, Phys. Rev. Lett. **76**, 212 (1996).
[14] S. H. Wei, J. Q. You, X. H. Yan, and X. G. Gong, J. Chem. Phys. **113**, 11127 (2000).
[15] J. Zhao, Q. Qiu, B. Wang, J. Wang, and G. Wang, Solid State Commun. **118**, 157 (2001).
[16] A. Taneda and Y. Kawazoe, Mater. Trans., JIM **41**, 635 (2000).
[17] M. Castro, S. R. Liu, H. J. Zhai, and L. S. Wang, J. Chem. Phys. **118**, 2116 (2003), following paper.
[18] L. S. Wang, H. S. Cheng, and J. Fan, J. Chem. Phys. **102**, 9480 (1995).
[19] X. Li, H. Wu, X. B. Wang, and L. S. Wang, Phys. Rev. Lett. **81**, 1909 (1998).
[20] L. S. Wang, J. Conceicao, C. Jin, and R. E. Smalley, Chem. Phys. Lett. **182**, 5 (1991).
[21] C. S. Feigerle, R. R. Corderman, S. V. Bobashev, and W. C. Lineberger, J. Chem. Phys. **74**, 1580 (1981).
[22] S. R. Liu, H. J. Zhai, and L. S. Wang, J. Chem. Phys. **117**, 9758 (2002).
[23] L. S. Wang, X. Li, and H. F. Zhang, Chem. Phys. **262**, 53 (2000).
[24] G. Gantefor and W. Eberhardt, Phys. Rev. Lett. **76**, 4975 (1996).
[25] S. Hufner, *Photoelectron Spectroscopy* (Springer-Verlag, New York, 1995).
[26] D. C. Douglass, J. P. Bucher, and L. A. Bloomfield, Phys. Rev. B **45**, 6341 (1992).
[27] D. M. Wood, Phys. Rev. Lett. **46**, 749 (1981).
[28] *Handbook of Chemistry and Physics*, 67th ed. (CRC, Boca Raton, FL, 1986).
[29] H. Wu, S. R. Desai, and L. S. Wang, Phys. Rev. Lett. **77**, 2436 (1996).
[30] L. S. Wang, H. Wu, and H. Cheng, Phys. Rev. B **55**, 12884 (1997).
[31] P. J. Feibelman and F. J. Himpsel, Phys. Rev. B **21**, 1394 (1980).
[32] D. M. Hanson, R. Stockbauer, and T. E. Madey, Phys. Rev. B **24**, 5513 (1981).
[33] I. Bakonyi, H. Ebert, and A. I. Liechtenstein, Phys. Rev. B **48**, 7841 (1993).
[34] A. Aguayo, G. Murrieta, and R. de Coss, Phys. Rev. B **65**, 092106 (2002).
[35] Y. Fukuda, G. M. Lancaster, F. Honda, and J. W. Rabalais, Phys. Rev. B **18**, 6191 (1978).